

Ab Initio Studies on Structural, Elastic, Thermodynamic and Electronic Properties of FeCrAs under Pressures

DE-CHUN HE^{a,*}, YONG PENG^a AND YONG-WEI HE^b

^aPhysical and Mechanical and Electrical Engineering College, Hexi University, Zhangye Gansu, 734000, China

^bInstitute of Atomic and Molecular Physics, Sichuan University, Chengdu 610065, China

(Received August 11, 2014; in final form February 10, 2015)

The structural, elastic, thermodynamic and electronic properties of nonmetallic metal FeCrAs are studied within density function perturbation theory. The thermodynamic properties of FeCrAs were deduced based on phonon frequencies within the framework of the quasiharmonic approximation. The calculated elastic modulus under various pressures indicates that FeCrAs is mechanically stable under pressure. The pressure-dependence of bulk and shear modulus, transverse and longitudinal sound velocities V (i.e. V_S and V_L), elastic Debye temperature Θ_E of FeCrAs have also been investigated. The calculated values of B/G indicate that FeCrAs presents high ductility under pressure. However, it is interesting that the value of B/G reaches a maximum under 40 GPa and almost remains unchanged when the pressure is above 70 GPa. The calculations show that the heat capacity C_V of this material is close to the Dulong–Petit limit $3R$ (about $224.61 \text{ J mol}^{-1} \text{ K}^{-1}$) at high temperature regime. The analysis of electronic properties find that as the pressure increases, the absolute value of charge for As and Fe atom increases while Cr remains nearly a constant, indicating that the mechanic properties of FeCrAs under pressure should be mostly attributed to the interaction between Fe and As atoms.

DOI: [10.12693/APhysPolA.127.1637](https://doi.org/10.12693/APhysPolA.127.1637)

PACS: 62.20.de, 65.40.Ba, 65.40.De, 72.15.-v

1. Introduction

Iron-pnictide compound FeCrAs, which is famous for its fantastic properties under temperatures and pressures, has attracted much theoretical effort in recent years [1–3]. Under low pressure (below 17 GPa), FeCrAs exhibits surprising property with Fermi-liquid-like specific heat but the resistivity shows strong non-metallic character and a breakdown of Fermi-liquid behavior. Such phenomenon also exists at quantum critical points of certain second-order phase-transition, such as heavy fermion criticality, Mott criticality and high- T_c cuprate phase transitions [4]. The fantastic properties of FeCrAs can be observed not only under pressures but also at temperatures, demonstrating that the resistivity of FeCrAs rises as the temperature falls at low temperature regime, but without a gap opening in the electronic excitation spectrum. Some of these behaviors have been successfully understood in the Kondo systems or disordered metals, which shows weak or strong localization according to whether they have high or low carrier densities. However, for some disordered heavy fermion compounds, such as FeCrAs studied in this work, the behaviors with respect to pressure and temperature are still under investigations.

Considering the exceptional behavior of resistivity for FeCrAs displaying under pressure and temperature, previous effort have been paid the emphasis on the optical, magnetism, and conductive properties of this compound [2, 5, 6]. Wu et al. [1] reported that when the

temperature is below 10 K, the resistivity follows a non-Fermi-liquid power law while the specific heat shows Fermi-liquid behavior with a large Sommerfeld coefficient. And the in-plane resistivity of FeCrAs shows an unusual “non-metallic” dependence on temperature T , rising continuously with decrease of T from 800 K to below 100 mK. Tafti et al. [2] found that the non-metallic behavior of FeCrAs is shown to be relatively unchanged under the pressure range of 0–17 GPa. Akrap et al. [3] studied the optical properties and electronic structure under ambient conditions and obtained that the optical conductivity has an anisotropic metallic character at room temperature. Specially, they also found that a low-frequency in-plane phonon mode decreases in frequency for $T < T_N$ (125 K), suggesting the possibility of spin-phonon coupling. Based on the BCS theory and previous investigations, the observing of the soft phonon modes in phonon dispersion curves often has special contribution to the superconductive properties of materials [7, 8]. Apart from above properties, the elastic, mechanic, lattice dynamic, thermodynamic and electronic properties under pressure and temperature also have crucial application in the further understanding of this material. For example, the study of elastic properties under pressure can provide important help on the further understanding of chemical bonds and cohesion of materials. On the other hand, knowledge of the thermodynamic properties of a crystal can provide essential insight into vibrational properties for the reason that the temperature dependence of heat capacity is governed by details of vibrations of the atoms and could only be determined from experiments for a long time. What is more, the phonon dispersion curves can provide a criterion for crystal dynamical stability and many other physical parameters of mate-

*corresponding author; e-mail: dechunhe@126.com

rials, such as thermodynamic constants, Grüneisen parameter γ , and superconducting transition temperature T_c , can be also obtained from phonon dispersion curves. Thus, the emphases of this work are placed on the elastic, mechanic, thermodynamic and electronic properties of FeCrAs at simultaneously high pressure and temperature.

In this work, our main aim is to investigate elastic, mechanic, thermodynamic and electronic properties of FeCrAs using density functional perturbation theory (DFPT). In Sect. 2 we describe our theoretical methods and the computation details briefly. In Sect. 3, the elastic, mechanic and thermodynamic properties of FeCrAs were deduced based on the obtained phonon frequencies within the framework of the quasiharmonic approximation (QHA). The main results and conclusions are summarized in Sect. 4. All of our work is implemented on Quantum-Espresso (QE) package [9], which is a very useful and credible tool based on the first-principles theory.

2. Methods and computational details

The elastic constants of FeCrAs was successfully obtained using the theoretical method proposed by Sin'ko and Smirnov. A brief description of this method is as follows: the lattice vectors \mathbf{a}' of the strained primitive cell are determined from the lattice vectors \mathbf{a} of the equilibrium primitive cell by the relation $\mathbf{a}' = \mathbf{a}(I + \hat{\varepsilon}_i)$, where I is the unit matrix and $\hat{\varepsilon}_i$ are strain tensors. To calculate five independent constants of hexagonal structures, we considered five independent volume-nonconserving strains, i.e.

$$\hat{\varepsilon}_1 = \begin{pmatrix} \gamma & 0 & 0 \\ 0 & 0 & 0 \\ 0 & 0 & \gamma \end{pmatrix}, \quad \hat{\varepsilon}_2 = \begin{pmatrix} \gamma & 0 & 0 \\ 0 & -\gamma & 0 \\ 0 & 0 & 0 \end{pmatrix}, \quad (1)$$

$$\hat{\varepsilon}_3 = \begin{pmatrix} \gamma & 0 & 0 \\ 0 & \gamma & 0 \\ 0 & 0 & 0 \end{pmatrix}, \quad \hat{\varepsilon}_4 = \begin{pmatrix} 0 & 0 & \gamma \\ 0 & 0 & 0 \\ \gamma & 0 & 0 \end{pmatrix}, \quad \hat{\varepsilon}_5 = \begin{pmatrix} 0 & 0 & 0 \\ 0 & 0 & 0 \\ 0 & 0 & \gamma \end{pmatrix}.$$

The specific energy of crystal deformed in accord with the $\hat{\varepsilon}_1$ was calculated as a function of the strain magnitude γ . The values of strain γ with the range of $\pm 5\%$ were used to make the strain energy fit to a second-order polynomial function. Then the strain energy as a function of the strain can be written as

$$C_{11} + 2C_{13} + C_{33} - 2P = \rho_1 \left. \frac{d^2 E(\rho_1, \hat{\varepsilon}_1)}{d\gamma^2} \right|_{\gamma=0}. \quad (2)$$

Here P was the pressure applied. Similar results with the order matrix were used in the equation

$$2(C_{11} - C_{12} - P) = \rho_1 \left. \frac{d^2 E(\rho_1, \hat{\varepsilon}_2)}{d\gamma^2} \right|_{\gamma=0}, \quad (3)$$

$$2(C_{11} + C_{12} - P) = \rho_1 \left. \frac{d^2 E(\rho_1, \hat{\varepsilon}_3)}{d\gamma^2} \right|_{\gamma=0}, \quad (4)$$

$$4C_{44} - 2P = \rho_1 \left. \frac{d^2 E(\rho_1, \hat{\varepsilon}_4)}{d\gamma^2} \right|_{\gamma=0}, \quad (5)$$

$$C_{33} - P = \rho_1 \left. \frac{d^2 E(\rho_1, \hat{\varepsilon}_5)}{d\gamma^2} \right|_{\gamma=0}. \quad (6)$$

The thermodynamic properties of FeCrAs were obtained based on the DFPT. In this method, the Helmholtz free energy of a system can be written as

$$F(V, T) = E_{\text{static}}(V) + F_{\text{el}}(V, T) + F_{\text{zp}}(V, T) + F_{\text{ph}}(V, T), \quad (7)$$

where $E_{\text{static}}(V)$ is the first-principles zero-temperature energy of a static lattice at volume V and $F_{\text{el}}(V, T)$ is the electronic free energy arising from the electronic thermal excitations at certain temperature T and volume V . $F_{\text{el}}(V, T)$ can be evaluated via the standard methods of finite-temperature DFT developed by Mermin (the Fermi-Dirac distribution) [10]:

$$F_{\text{el}}(V, T) = E_{\text{el}}(V, T) - TS_{\text{el}}(V, T). \quad (8)$$

The electronic energy arising from the electronic excitations can be given as

$$E_{\text{el}}(V, T) = \int n(\varepsilon) f(\varepsilon) \varepsilon d\varepsilon - \int^{\varepsilon_F} n(\varepsilon) \varepsilon d\varepsilon, \quad (9)$$

where $n(\varepsilon)$ is the electronic density of states (EDOS) at the energy eigenvalue ε , f is the Fermi distribution function, and ε_F is the energy at the Fermi level.

The electronic entropy is calculated by

$$S_{\text{el}}(V, T) = -2k_B \sum_{f_i} \ln f_i + (1 - f_i) \ln(1 - f_i). \quad (10)$$

Here k_B is the Boltzmann constant.

The term $F_{\text{zp}}(V, T)$ in Eq. (7) is the zero-point motion energy of the lattice given by

$$F_{\text{zp}} = \frac{1}{2} \sum_{q,j} \hbar \omega_j(q, V), \quad (11)$$

where $\omega_j(q, V)$ is the phonon frequency of the j -th mode of wave vector \mathbf{q} in the first Brillouin zone (BZ).

The last term in Eq. (7) is the phonon free energy due to lattice vibrations, and it can be expressed as

$$F_{\text{ph}}(V, T) = k_B T \times \sum_{q,j} \ln(1 - \exp(-\hbar \omega_j(q, V)/k_B T)). \quad (12)$$

The calculation of phonon dispersion curves of FeCrAs were calculated within DFPT [11, 12] using local-density approximation [13] with the parametrization of the Perdew and Zunger [14]. A nonlinear core correction to the exchange-correlation energy function was introduced to generate a norm-conserving pseudopotential [15] for Fe, Cr, and As with the valence electrons configuration $3d^6 4s^2$, $3s^2 3p^6 3d^5 4s^1$, and $4s^2 4p^3$, respectively. To ensure the convergence of the free energy and phonon frequencies, a careful test was made on k and q grids, as well as the kinetic energy cutoff and smearing parameters. For the hexagonal FeCrAs, dynamical matrices were computed at 8 wave (q) vectors using a $4 \times 4 \times 3$ grid in the irreducible wedge of the Brillouin zone. The plane wave cutoff for the wave functions was 60 Ry. The Monkhorst-Pack (MP) meshed were $16 \times 16 \times 12$ and the Fermi-Dirac smearing width was 0.02 Ry.

3. Results and discussion

3.1. Structural and elastic properties

FeCrAs has a hexagonal structure [space group $P\bar{6}m2$ (No. 187)] and the Fe and Cr atoms occupy the sides ($x, 0, 1/2$) and ($z, 0, 0$) with $x = 0.2505$ and $z = 0.5925$, respectively. The positions of As atoms are at (0,0,0) and (1/3,2/3,1/2). To reach the structure optimization, the volume V and the c/a ratios were optimized. Since the experimental c/a ratio of FeCrAs is about 0.599 [3], a series of different c/a ratio were calculated between 0.50 and 0.70 with a step of 0.001. For each fixed value of c/a , a series of different values of a and c are taken to calculate the total energies E and corresponding volumes V . Then an energy–volume (E – V) curve can be obtained by fitting the calculated E – V results to the Birch–Murnaghan equation of states (EOS) [16], in which the pressure–volume relationship expanded to the fourth-order in strain is

$$P = 3B_0 f_E (1 + f_E)^{5/2} \left\{ 1 + \frac{3}{2}(B' - 4)f_E + \frac{3}{2} \left[B_0 B'' + (B' - 4)(B' - 3) + \frac{35}{9} f_E^2 \right] f_E^2 \right\}, \quad (13)$$

where f_E is written as

$$f_E = [(V_0/V)^{2/3} - 1]/2. \quad (14)$$

In Fig. 1, we illustrate some of the fitted E – V curves of various c/a ratios. It is found that the E – V curve with the ratio c/a of about 0.597 has the minimum energy, and the corresponding equilibrium lattice parameters c and a are about 3.548 and 5.943 Å, respectively. The calculated results combined with experimental data and other theoretical results are given in Table I. Compared with the experimental data [17–19], the calculated lattice parameters are underestimated slightly (about 2.8% for c and 2.5% for a). The difference is reasonable for the reason that experiments are implemented under ambient conditions while the effects of temperature are not

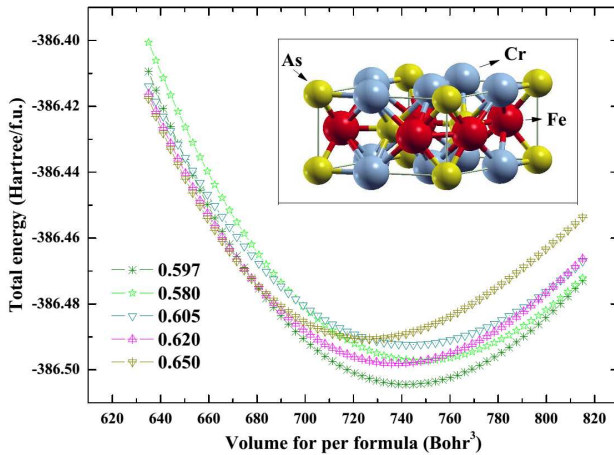


Fig. 1. The total energy E of FeCrAs as a function of primitive cell volume V for different axial ratios c/a . The inside graphic is the molecular structure model of FeCrAs.

TABLE I

The calculated structure parameters, bulk modulus B_0 and its pressure derivation B'_0 at 0 GPa and 0 K compared with other experimental and theoretical data.

	a	c	c/a	B_0	B'_0
	[Å]			[GPa]	
Present work	5.943	3.548	0.597	228.66	4.6547
Theory*	5.989	3.609	0.602		
Experiment**	6.096	3.651	0.598		

*Ref. [3] GGA using FP-LAPW method by WIEN2k code.

**Ref. [17–19] ambient conditions.

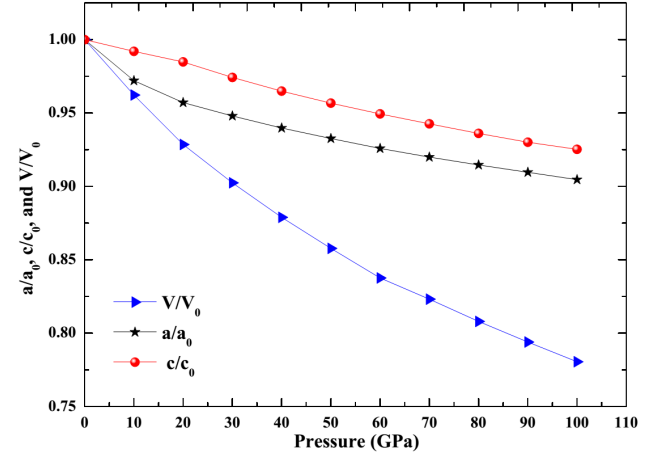


Fig. 2. The normalized parameters a/a_0 , c/c_0 , and V/V_0 of FeCrAs as a function of pressure at 0 K.

considered in first-principles calculations. Based on the obtained EOS using Eq. (13), one can obtain the fitted lattice parameters of c and a are about 6.087 and 3.637 at 273 K, agreeing well with experimental results. From Table I, it can be seen that the calculated zero pressure bulk modulus B_0 and its pressure derivation B'_0 from the Birch–Murnaghan EOS are about 228.66 GPa and 4.6547 at 0 K, respectively. The pressure dependence of the normalized lattice parameters a/a_0 , c/c_0 , and the normalized primitive cell volume V/V_0 of FeCrAs (where a_0 , c_0 , and V_0 are the zero pressure equilibrium structure parameters) are illustrated in Fig. 2. It is shown that with increasing pressure, the equilibrium ratio a/a_0 decreases more quickly compared with c/c_0 , indicating that the compression along a -axis is larger. In the pressure range of 0–100 GPa, the basal plane linear $d(\ln a)/dP = 0.001003 \text{ GPa}^{-1}$ is 1.291 times greater than the interlayer value $d(\ln c)/dP = 0.000777 \text{ GPa}^{-1}$, which suggests that a -axis is more sensitive to pressure than the c -axis.

3.2. Elastic properties

It is known that the elastic constants C_{11} (C_{33}) are related to the elasticity in length, while the elastic constants C_{12} (C_{13}) and C_{44} (C_{66}) represent the elasticity in shape. For FeCrAs, it is found that C_{11} , C_{12} , C_{13} , and C_{33} are susceptible to pressure, while the variation of C_{44}

and C_{66} are slow with increasing pressure (Fig. 3). However, there exists a minimum under 40 GPa for C_{66} . The calculations also indicate that the atomic bonds along (001) plane between nearest neighbors are stronger than those along (100) plane. Another striking feature of the elastic constants for FeCrAs is that C_{11} , C_{12} , C_{13} , and C_{33} present fluctuate characters under pressure. Based on the obtained elastic constants, the bulk modulus along a -axis (B_a) and c -axis (B_c) can be defined as follows to qualify the mechanical anisotropy of FeCrAs [20] *i.e.*:

$$B_a = a \frac{dP}{da} = \frac{A}{2 + \alpha}, \quad (15)$$

$$B_c = c \frac{dP}{dc} = \frac{B_a}{\alpha}, \quad (16)$$

$$A = 2(C_{11} + C_{12}) + 4C_{13}\alpha + C_{33}\alpha^2, \quad (17)$$

$$\alpha = \frac{C_{11} + C_{12} - 2C_{13}}{C_{33} - C_{13}}. \quad (18)$$

The five independent elastic constants combined with bulk modulus B_a and B_c under pressures are given in Table II. It should be noted that B_c is much larger than B_a under 0 GPa and above ambient pressure, B_a and B_c present an increasing trend with pressure. However, B_a becomes higher than B_c in the pressure range of 10–60 GPa. Then B_a reaches a maximum with 2191.8 GPa under 90 GPa, while the maximum of B_c is 2546.1 GPa when pressure is 70 GPa. For a hexagonal structure, the mechanical stability under isotropic pressures can be estimated from criterion as follows [21]:

$$\tilde{C}_{44} > 0, \quad \tilde{C}_{11} > |\tilde{C}_{12}|, \quad \tilde{C}_{33}(\tilde{C}_{11} + \tilde{C}_{12}) > 2\tilde{C}_{13} \quad (19)$$

in which $\tilde{C}_{\alpha\alpha} = C_{\alpha\alpha} - P$ ($\alpha = 1, 4$), $\tilde{C}_{12} = C_{12} + P$, $\tilde{C}_{13} = C_{13} + P$. The elastic constants of FeCrAs given in Table II all satisfy these stability conditions, indicating the mechanical stable of FeCrAs.

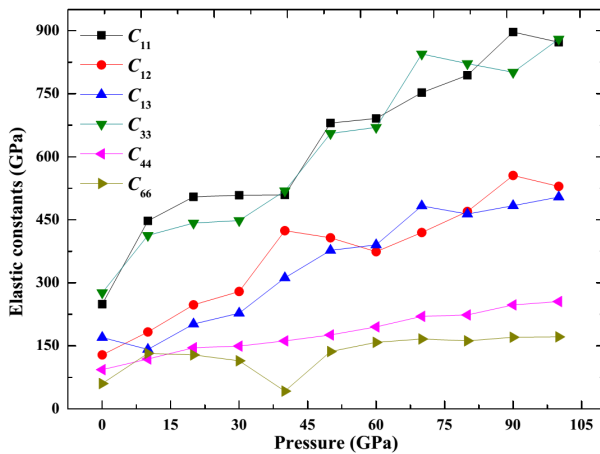


Fig. 3. Pressure dependence of elastic constants of FeCrAs at 0 K.

The isotropic bulk modulus B_V and shear modulus G_V for a hexagonal crystal can be expressed as

TABLE II

Calculated elastic constants C_{ij} [GPa] of FeCrAs in the pressure range of 0-100 GPa, as well as bulk modulus B_a and B_c .

P	C_{11}	C_{12}	C_{13}	C_{33}	C_{44}	C_{66}	B_a	B_c
0	249.3	128.5	170.1	276.5	93.5	60.4	437.9	1239.2
10	447.6	183.1	141.7	413.1	118.9	132.2	812.0	634.6
20	504.8	247.7	202.1	442.4	145.6	128.5	1045.4	721.3
30	508.6	279.4	227.9	448.3	149.5	114.6	1131.5	750.7
40	509.2	424.2	312.0	519.0	161.9	42.5	1399.7	936.5
50	680.4	407.2	377.4	655.6	176.1	136.6	1539.1	1286.6
60	691.3	374.2	390.4	670.2	195.4	158.6	1462.7	1437.6
70	752.1	419.7	483.2	844.8	220.4	166.5	1446.3	2546.1
80	794.1	469.9	463.8	821.8	223.8	162.1	1699.8	1808.9
90	896.9	555.6	483.7	801.1	247.7	170.6	2191.8	1434.1
100	872.7	529.6	504.3	880.1	255.6	171.6	1930.6	1842.8

TABLE III

Calculated bulk modulus B [GPa], shear modulus G [GPa], sound velocities V_S , V_L , V_M [m/s] and elastic Debye temperature Θ_E of FeCrAs under pressure.

P	B	G	B/G	V_S	V_L	V_M	Θ_E
0	186.1	66.59	2.7947	2423.8	4924.2	2721.5	349.4
10	247.6	129.6	1.9105	3266.3	5882.4	3637.9	478.0
20	303.1	136.9	2.2140	3301.4	6217.3	3689.3	490.2
30	322.6	130.3	2.4758	3173.1	6192.4	3554.3	477.0
40	400.5	89.8	4.4599	2598.8	6254.5	2940.1	398.2
50	481.5	153.7	3.1327	3359.0	7099.1	3779.5	515.9
60	484.7	168.3	2.8799	3476.4	7135.9	3905.7	537.1
70	563.2	183.3	3.0726	3591.4	7539.0	4039.6	559.2
80	578.2	187.4	3.0854	3597.9	7563.3	4047.2	563.8
90	621.8	201.5	3.0859	3699.1	7772.9	4160.9	582.9
100	633.5	205.6	3.0812	3706.1	7786.3	4168.9	587.3

TABLE IV

Mulliken populations of FeCrAs under different pressures.

Pressure [GPa]	Atoms	s	p	d	Total	Charge transfer [e]
0	Cr	2.59	6.90	5.15	14.65	-0.65
	Fe	0.48	0.72	6.97	8.17	-0.17
	As	0.83	3.35	0.00	4.18	0.82
30	Cr	2.61	6.88	5.18	14.68	-0.68
	Fe	0.49	0.71	6.99	8.18	-0.18
	As	0.78	3.35	4.13	4.13	0.87
60	Cr	2.63	6.83	5.22	14.68	-0.68
	Fe	0.51	0.68	7.02	8.21	-0.21
	As	0.73	3.35	0.00	4.08	0.92
90	Cr	2.65	6.76	5.25	14.67	-0.67
	Fe	0.54	0.66	7.04	8.24	-0.24
	As	0.70	3.35	0.00	4.05	0.95

$$B_V = \frac{1}{9}[2(C_{11} + C_{12}) + C_{33} + 4C_{13}], \quad (20)$$

$$G_V = \frac{1}{30}(C_{11} + C_{12} + 2C_{33} - 4C_{13} + 12C_{44} + 12C_{66}). \quad (21)$$

The isotropic bulk modulus B_R and shear modulus G_R are given by:

$$B_R = \frac{(C_{11} + C_{12})C_{33} - 2C_{13}^2}{C_{11} + C_{12} + 2C_{33} - 4C_{13}}, \quad (22)$$

$$G_R = \frac{5}{2} \left\{ [(C_{11} + C_{12})C_{33} - 2C_{13}^2]^2 C_{44} C_{66} \right\} / \left\{ 3B_V C_{44} C_{66} + [(C_{11} + C_{12})C_{33} - 2C_{13}^2]^2 (C_{44} + C_{66}) \right\}. \quad (23)$$

Here

$$C_{66} = \frac{1}{2}(C_{11} - C_{12}). \quad (24)$$

The average of the Voigt and Reuss bulk modulus is called as the Voigt–Reuss–Hill (VRH) average and can be commonly used to estimate elastic modulus of polycrystals. The VRH average for shear modulus (G) and bulk modulus (B) are defined as:

$$G = \frac{1}{2}(G_R + G_V), \quad B = \frac{1}{2}(B_R + B_V). \quad (25)$$

Then the values of the average transverse and longitudinal sound velocities can be calculated from the Navier equation [22]:

$$V_S = \sqrt{\frac{G}{\rho}}, \quad V_L = \sqrt{\frac{B + \frac{4}{3}G}{\rho}}. \quad (26)$$

Based on above sound velocities, the elastic Debye temperature Θ_E can be obtained from the average sound velocity V_m [23]:

$$\Theta_E = \frac{h}{k} \left[\frac{3n}{4\pi} \left(\frac{\rho N_a}{M} \right) \right]^{\frac{1}{3}} V_m. \quad (27)$$

Where h is the Planck constant, k is the Boltzmann constant, N_a is the Avogadro number, and n is the number of atoms per formula unit, M is the molecular mass per formula unit. ρ is the density and V_M can be obtained by [23]:

$$V_M = \left[\frac{1}{3} \left(\frac{2}{V_S^3} + \frac{1}{V_L^3} \right) \right]^{-\frac{1}{3}}. \quad (28)$$

The calculated results for bulk modulus B [GPa], shear modulus G [GPa], and sound velocities V_S, V_L, V_M , as well as elastic Debye temperature Θ_E of FeCrAs under pressure are illustrated in Table III. Generally, the bulk modulus and shear modulus are used to measure the hardness of materials. In the studied pressure range, one can find that the bulk modulus B increases gradually with the increase of pressure, indicating that FeCrAs becomes more and more difficult to compress with increasing pressure. It should be noticed here FeCrAs has a relative high bulk modulus (above 400 GPa when $P > 40$ GPa) under pressure since it is known that the bulk modulus of diamond is 434 GPa under ambient conditions [24]. Simultaneously, the ratio of bulk modulus and shear modulus, i.e. B/G , has been applied to estimate the ductile or brittle properties of materials. The value of B/G that separates ductile and brittle of mate-

rials is about 1.75. In Table III, the calculated values of B/G are all higher than above value, indicating that FeCrAs presents high ductility under pressure. However, it is interesting that the value of B/G reaches a maximum under 40 GPa and almost remains unchanged when the pressure is above of 70 GPa. This phenomenon demonstrates that the pressure can improve a material's ductility in a certain pressure range.

3.3. Thermodynamic properties

The accurate thermodynamic properties as a function of pressure and temperature can directly provide the valuable information for understanding the dynamical response of materials under extreme conditions. The thermodynamic properties of FeCrAs were obtained within the quasi-harmonic approximation (QHA) theory. In the framework of QHA theory, the Helmholtz free energy as a function of volume V and temperature T can be derived after taking into account the thermal electronic excitation and phonon contributions. In order to deduce the thermodynamic properties, we fitted a fourth-order finite-strain EOS [25] to the calculated free energy versus volume at each temperature. The fitted isothermal compressional curves are given in Fig. 4. It can be seen that, as the pressure increases, the relative volume V/V_0 decreases at a given temperature, and the relative volume V/V_0 of higher temperature is less than that of lower temperature at the same pressure. On the other hand, the volume V decreases with the increasing pressure P , and increases with the elevation of temperature T , indicating that the effect of increasing pressure on FeCrAs is the same as decreasing temperature.

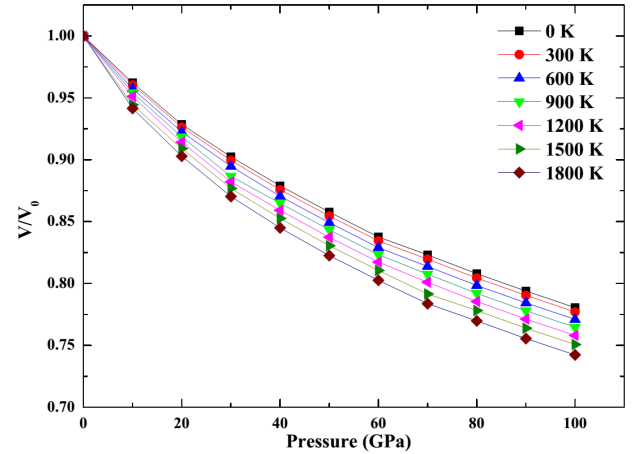


Fig. 4. The isothermal compressional curves at different temperatures. V_0 denotes the incipient volume of FeCrAs at the pressure of 0 GPa.

The thermal expansion coefficient

$$\alpha_V = \frac{1}{V} \left(\frac{\partial V}{\partial T} \right)_P \quad (29)$$

can be obtained from the equilibrium volume variation with respect to the temperature at each pressure. In Fig. 5a and b, the thermal expansion coefficient as functions of temperature and pressure are plotted. At a given

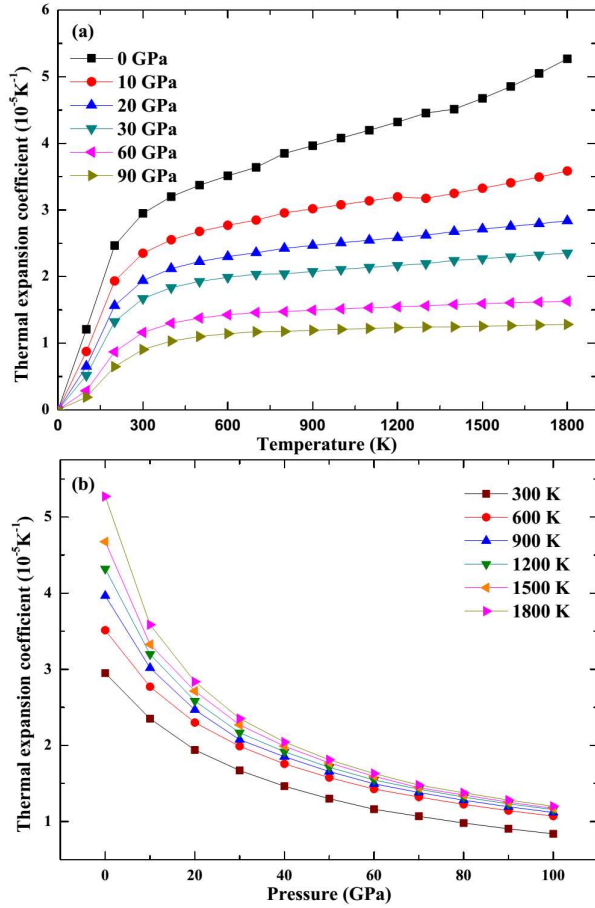


Fig. 5. Thermal expansion coefficient versus temperature (a) and pressure (b) of FeCrAs.

pressure, α increases exponentially at low temperatures and gradually approaches a linear increase at high temperature range. As the pressure increases, the increase of α with temperature becomes smaller, especially at high temperatures. However, α decreases drastically with the increase of pressure at a given temperature. On the other hand, the difference of thermal expansion α at high temperature tends to be smaller compared with that of at low temperature and the curves seem to be parallel to each others, which means that the temperature-dependence of thermal expansion coefficient is small at high temperature.

The specific heat at constant volume is defined as

$$C_V = \left(\frac{\partial U}{\partial T} \right)_V, \quad (30)$$

where U is the internal energy of the whole system. The specific heat at constant pressure C_P is different from C_V due to the thermal expansion caused by anharmonic effects. The relation between C_P and C_V can be described by the following relations:

$$C_P - C_V = \alpha_V(T)B_0VT. \quad (31)$$

Here α_V is the volume thermal expansion coefficient. B_0 is the bulk modulus and T is the temperature, while V is the volume. It is known that C_V increases dramati-

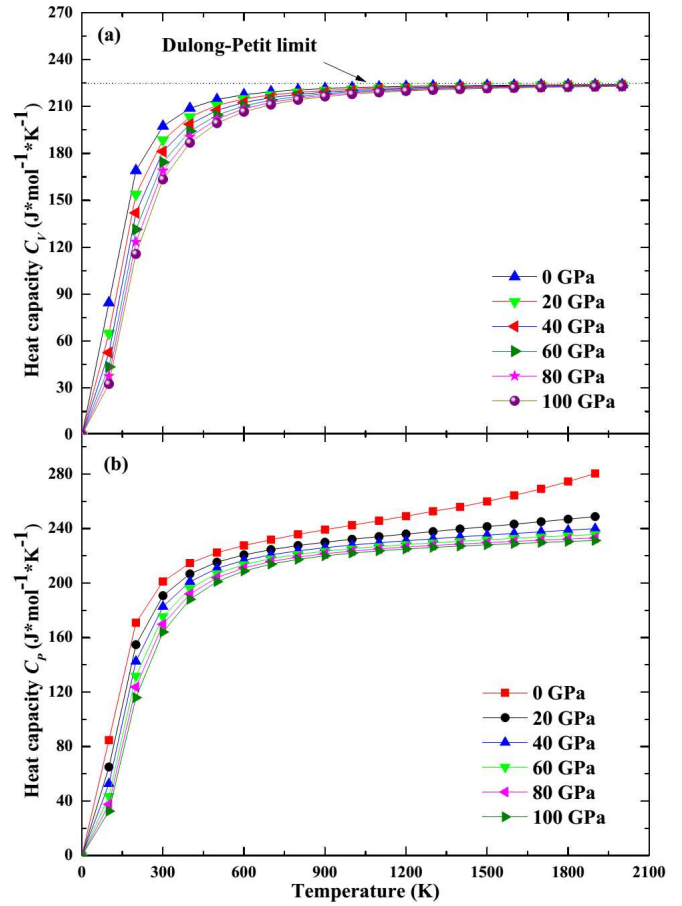


Fig. 6. Calculated constant volume heat capacity C_v (a) and C_p (b) of FeCrAs as a function of temperature under different pressures. The dotted line displayed in (a) represents Dulong–Petit limit.

cally as temperature increases and finally approaches a constant $3R$. From Eq. (31), there can be seen the C_P of FeCrAs as a function of temperature at different pressures. As far as we know, there are few studies have been reported on the C_V and C_P of FeCrAs, thus we present our calculations in Fig. 6. When $T < 1200$ K, the heat capacity C_V is dependent on both temperature T and pressure P . These relations can be attributed to the effect of anharmonic approximations for materials. However, the heat capacity C_V is close to the Dulong–Petit limit $3R$ (about $224.61 \text{ J mol}^{-1} \text{ K}^{-1}$) at higher temperatures (> 1200 K), presenting a common phenomenon to all solids at high temperatures. On the other hand, the heat capacity decreases more quickly with increasing pressure at low temperature compared with that at high temperature. At a given pressure, C_P increases exponentially at low temperatures and gradually turns to a line-increase mode at high-temperature regime. As the pressure increases, C_P decreases at a given temperature.

3.4. Electronic properties under pressure

To investigate the pressure dependence of electronic properties for FeCrAs, the Mulliken charges [26] are calculated under different pressures. The Mulliken charge

$Q_m(A)$ of A atom and the overlap population $n_m(AB)$ for $A-B$ bond are defined as follows:

$$Q_m(A) = \sum_k W(k) \sum_v^A P_{uv}(k) S_{uv}(k), \quad (32)$$

$$n_m(AB) = \sum_k W(k) \sum_u^A \sum_v^B P_{uv}(k) S_{uv}(k). \quad (33)$$

Here $P_{uv}(k)$ and $S_{uv}(k)$ are the density matrix and the overlap matrix, respectively. u and v are the orbitals on A and B , respectively. $W(k)$ is the weight associated the calculated k points in the Brillouin zone. Generally, the magnitude and sign of $Q_m(A)$ characterized the iconicity of A atom in the crystal, and $n_m(AB)$ can be used to measure the covalent bonding strength approximately. The calculated Mulliken populations of FeCrAs obtained under different pressures are listed in Table IV. From Table IV, it can be deduced that As loses electrons while Fe and Cr present negative values under pressures. As the pressure increases, the absolute value of charge for As and Fe atom increases while Cr remains nearly a constant. This indicates that the mechanic properties of FeCrAs under pressure should be mostly attributed to the interaction between Fe and As atoms.

4. Conclusions

In summary, the structural, elastic, thermodynamic and electronic properties of the novel nonmetallic metal FeCrAs under high pressure are investigated within density function theory. The pressure-dependence of the elastic constants, elastic modulus, transverse and longitudinal sound velocities V (i.e. V_S and V_L), and elastic Debye temperature Θ_E of FeCrAs have also been obtained firstly. The calculated elastic modulus at various pressures indicates FeCrAs is mechanically stable under pressure. It is also reasonable to deduce that FeCrAs has a relative high bulk modulus under pressure based on the knowledge that the bulk modulus of diamond is 434 GPa under ambient conditions. The calculated values of B/G indicate that FeCrAs presents high ductility under pressure. However, it is interesting that the value of B/G reaches a maximum under 40 GPa and almost remains unchanged when the pressure is above of 70 GPa. The calculations show that the heat capacity C_V of this material is close to the Dulong–Petit limit $3R$ (about $224.61 \text{ J mol}^{-1} \text{ K}^{-1}$) at high temperature regime. The analysis of electronic properties finds that as the pressure increases, the absolute value of charge for As and Fe atom increases while Cr remains nearly a constant, indicating that the mechanic properties of FeCrAs under pressure should be mostly attributed to the interaction between Fe and As atoms.

Acknowledgments

We acknowledge the support for the computational resources by the State Key Laboratory of Polymer Materials Engineering of China in Sichuan University.

References

- [1] W. Wu, A. McCollam, I. Swainson, P.M.C. Rourke, D.G. Rancourt, S.R. Julian, *Euro. Phys. Lett.* **85**, 17009 (2009).
- [2] F.F. Tafti, W. Wu, S.R. Julian, *J. Phys. Condens. Matter* **25**, 385601 (2013).
- [3] A. Akrap, Y.M. Dai, W. Wu, S.R. Julian, C.C. Homes, *Phys. Rev. B* **89**, 125115 (2014).
- [4] T. Senthil, *Phys. Rev. B* **78**, 035103 (2008).
- [5] J.G. Rau, H.Y. Kee, *Phys. Rev. B* **84**, 104448 (2011).
- [6] J.M. Florez, P. Vargas, C. Garcia, C.A. Ross, *J. Phys. Condens. Matter* **25**, 226004 (2013).
- [7] J.S. Tse, Y. Yao, K. Tanaka, *Phys. Rev. Lett.* **98**, 117004 (2007).
- [8] Y.K. Wei, N.N. Ge, G.F. Ji, X.R. Chen, L.C. Cai, S.Q. Zhou, D.Q. Wei, *J. Appl. Phys.* **114**, 114905 (2013).
- [9] P. Giannozzi, S. Baroni, N. Bonini, M. Calandra, R. Car, C. Cavazzoni, D. Ceresoli, G.L. Chiarotti, M. Cococcioni, I. Dabo, A. Dal Corso, S. de Gironcoli, S. Fabris, G. Fratesi, R. Gebauer, U. Gerstmann, C. Gougoussi, A. Kokalj, M. Lazzeri, L. Martin-Samos, N. Marzari, F. Mauri, R. Mazzarello, S. Paolini, A. Pasquarello, L. Paulatto, C. Sbraccia, S. Scandolo, G. Sclauzero, A.P. Seitsonen, A. Smogunov, P. Umari, R.M. Wentzcovitch, *J. Phys. Condens. Matter* **21**, 395502 (2009).
- [10] N.D. Mermin, *Phys. Rev.* **137**, A1441 (1965).
- [11] S. Baroni, P. Giannozzi, A. Testa, *Phys. Rev. Lett.* **58**, 1861 (1987).
- [12] S. Baroni, S.D. Gironcoli, A.D. Corso, P. Giannozzi, *Rev. Mod. Phys.* **73**, 515 (2001).
- [13] W. Kohn, L.J. Sham, *Phys. Rev. B* **140**, A1133 (1965).
- [14] J.P. Perdew, A. Zunger, *Phys. Rev. B* **23**, 5048 (1981).
- [15] B. Hammer, I.B. Hansen, J.K. Norskov, *Phys. Rev. B* **59**, 7413 (1999).
- [16] F. Birch, *Phys. Rev.* **71**, 809 (1947).
- [17] L. Hollan, *Ann. Chim. (Paris)* **1**, 437 (1966).
- [18] M. Nyland, M. Roger, J. Sénateur, R. Fruchart, *J. Solid State Chem.* **4**, 115 (1972).
- [19] R. Guérin, M. Sergent, *Mater. Res. Bull.* **12**, 381 (1977).
- [20] P. Ravindran, L. Fast, P.A. Korzhavyi, B. Johansson, J. Wills, O. Eriksson, *J. Appl. Phys.* **84**, 4891 (1998).
- [21] G.V. Sin'ko, N.A. Smirnov, *J. Phys. Condens. Matter* **14**, 6989 (2002).
- [22] R. Hill, *Proc. Soc. Lond. A* **65**, 349 (1952).
- [23] O.L. Anderson, *J. Phys. Chem. Solids* **21**, 909 (1963).
- [24] K.B. Panda, K.S. Ravi Chandran, *Comput. Mater. Sci.* **35**, 134 (2006).
- [25] F. Birch, *J. Geophys. Res.* **91**, 4949 (1986).
- [26] R.S. Mulliken, *J. Chem. Phys.* **45**, 1833 (1955).